Eur Respir J 2001; 17: 1167–1174
Printed in UK – all rights reserved

European Respiratory Journal
ISSN 0903-1936

Noninvasive measurement of mean alveolar carbon dioxide tension and Bohr's dead space during tidal breathing

N.G. Koulouris, P. Latsi, J. Dimitroulis, B. Jordanoglou, M. Gaga, J. Jordanoglou

Noninvasive measurement of mean alveolar carbon dioxide tension and Bohr's dead space during tidal breathing. N.G. Koulouris, P. Latsi, J. Dimitroulis, B. Jordanoglou, M. Gaga, J. Jordanoglou. ©ERS Journals Ltd 2001.

ABSTRACT: The lack of methodology for measuring the alveolar carbon dioxide tension (P_{A,CO_2}) has forced investigators to make several assumptions, such as that P_{A,CO_2} is equal to end-tidal (P_{ET,CO_2}) and arterial CO_2 tension (P_{a,CO_2}).

The present study measured the mean P_{A,CO_2} and Bohr's dead space ratio (Bohr's dead space/tidal volume ($V_{D,Bohr}/V_T$)) during tidal breathing. The method used is a new, simple and noninvasive technique, based on the analysis of the expired CO_2 volume per breath (V_{CO_2}) *versus* the exhaled V_T. This curve was analysed in 21 normal, healthy subjects and 35 chronic obstructive pulmonary disease (COPD) patients breathing tidally through a mouthpiece apparatus in the sitting position.

It is shown that: 1) P_{A,CO_2} is similar to P_{a,CO_2} in normal subjects, whilst it is significantly lower than P_{a,CO_2} in COPD patients; 2) P_{A,CO_2} is significantly higher than P_{ET,CO_2} in all subjects, especially in COPD patients; 3) $V_{D,Bohr}/V_T$ is increased in COPD patients as compared to normal subjects; and 4) $V_{D,Bohr}/V_T$ is lower than the "physiological" dead space ratio ($V_{D,phys}/V_T$) in COPD patients.

It is concluded that the expired carbon dioxide *versus* tidal volume curve is a useful tool for research and clinical work, because it permits the noninvasive and accurate measurement of Bohr's dead space and mean alveolar carbon dioxide tension accurately during spontaneous breathing.

Eur Respir J 2001; 17: 1167–1174.

Dept of Respiratory Medicine, Respiratory Function Laboratory, University of Athens Medical School, "Sotiria" Hospital for Diseases of the Chest, Athens, Greece.

Correspondence: J. Jordanoglou, Dept of Respiratory Medicine, Respiratory Function Laboratory, University of Athens Medical School, "Sotiria" Hospital for Diseases of the Chest, 152, Mesogion Ave, Athens, GR-11527, Greece
Fax: .30 17770423

Keywords: Alveolar carbon dioxide tension
arterial carbon dioxide tension
Bohr's dead space
chronic obstructive pulmonary disease
end-tidal carbon dioxide
physiological dead space

Received: July 13 2000
Accepted after revision January 30 2001

The respiratory dead space is the concept in gas exchange derived by the investigators in their effort to determine the effectiveness of ventilation in health and disease. After the description of the dead space by BOHR [1], numerous papers on the subject followed, in which the methodology can be divided into two categories; the noninvasive studies from gas (nitrogen (N_2), Helium (He), carbon dioxide (CO_2)) concentration *versus* time or volume curves, and the invasive studies in which the arterial CO_2 tension (P_{a,CO_2}) instead of the alveolar CO_2 tension (P_{A,CO_2}) was used [2–15]. In the noninvasive methods, the "anatomical" dead space, *i.e.* Fowler's dead space ($V_{D(F)}$), is determined from the expired gas concentration *versus* tidal volume or vital capacity curve, which is analysed by geometrical methods. The results obtained by this method may be doubtful since the junction of the phases II and III is difficult to define in disease, especially during tidal breathing. Furthermore, this analysis is based on the assumption that the end-tidal and alveolar CO_2 fractions (F_{ET,CO_2} and F_{A,CO_2}) are identical. However, there is substantial evidence that F_{ET,CO_2} is lower than F_{A,CO_2} in normal subjects and patients [16–18]. The invasive methods permit the measurement of the "physiological" dead space ratio (physiological dead space/tidal volume ($V_{D,phys}/V_T$)), by using P_{a,CO_2} in Bohr's equation with the assumption that P_{A,CO_2} is equal to P_{a,CO_2}, which is valid only in normal subjects.

In previous reports [17, 18], Bohr's dead space ratio (Bohr's dead space/tidal volume ($V_{D,Bohr}/V_T$)) and P_{A,CO_2} were not measured either simultaneously or within the volume domain. Since $V_{D,Bohr}/V_T$ is in the volume domain, theoretically it appeared most appropriate to develop a new technique, *i.e.* the construction and mathematical analysis of the expired CO_2 volume *versus* tidal volume curve (V_{CO_2} *versus* V_T curve). This curve, recorded at the mouth during expiration, has a curvilinear shape and the CO_2 concentrations within the airways are lower than the alveolar one as a result of the "dilution effect" due to the pre-inspired atmospheric air (Appendix 1).

This technique allowed the simultaneous measurement of $V_{D,Bohr}/V_T$ and P_{A,CO_2}. This simple and noninvasive method was applied in 21 normal subjects and 35 chronic obstructive pulmonary disease (COPD) patients breathing tidally through a mouthpiece apparatus. $V_{D,Bohr}/V_T$ was compared to $V_{D,phys}/V_T$, and P_{A,CO_2} to P_{a,CO_2} and end-tidal carbon dioxide tension (P_{ET,CO_2}).

Methods

Theoretical considerations

The $V\dot{C}O_2$ *versus* VT curve was derived from the expiratory flow and CO_2 concentration *versus* time tracings measured at the mouth. It was constructed by plotting the exhaled $V\dot{C}O_2$ (the integral of CO_2 fraction and flow with respect to time ($V\dot{C}O_2=\int F\dot{C}O_2\ V'dt$)) *versus* the tidal volume (the integral of flow with respect to time ($V\text{T}=\int V'dt$)). The F_{ET,CO_2} was determined, by computer analysis, from the mean of 10 points of the last segment on the $F\dot{C}O_2$ *versus* time curve, at which the positive slope of the tangent with the horizontal line becomes zero. Beyond these points the curve started to have a consistent negative slope. The height of the mean of these points from the zero line of the curve represents the F_{ET,CO_2}. The mixed expired CO_2 fraction (F_{E,CO_2}) is the ratio of the total expired $V\dot{C}O_2$ per breath over VT (Appendix 1). The analysis of the $V\dot{C}O_2$ *versus* VT curve is described in detail in the Appendix section.

Study design

The experimental set-up consisted of a flanged semirigid plastic mouthpiece connected in series to a Fleisch No. 2 flow transducer head (Fleisch, Lausanne, Switzerland) *via* a metal piece (monitoring ring), on which the CO_2 probe was attached (mouthpiece apparatus). The pneumotachograph (transducer and amplifier: Gould, Godart BV; No. 17212, Bilthoven, Holland) was connected with the Fleisch head *via* two semirigid plastic tubes 50 cm in length. The pneumotachograph system (rise time 10–90%=13 ms) was linear over the range of flows used. Volume was obtained by integration of the flow signal. An infrared capnograph (Jaeger; CO_2 test III, Wuerzburg, Germany) (rise time 10–90%=100 ms) was connected to the monitoring ring through a thin polythene tube (length 50 cm, internal diameter 1.2 mm). The resistance of the mouthpiece apparatus to airflow was negligible. The rise time (10–90%) of the capnograph measured at the mouthpiece was $\geqslant$4.5 times faster than that of the fastest $F\dot{C}O_2$ *versus* time curve ($F\dot{C}O_2/t$), in normal subjects and COPD patients breathing at a frequency of 10–25·min^{-1}. Calibration of the CO_2 analyser was made using a standard mixture of CO_2 (4.0%) in N_2. The phase lag between the $F\dot{C}O_2$ *versus* t and V' *versus* t signals was determined by an abrupt change in flow of the above gas mixture generated through the experimental set-up. The measurement of the phase lag and the calibration of the CO_2 analyser were repeated three times and the mean values were used. Airflow and CO_2 signals were monitored on-line on a computer screen and sampled simultaneously at a rate of 150 Hz using a computer data acquisition system with a built-in 12-bit analogue-to-digital converter (National Instruments, AT-M10, Austin, Texas, USA). Collected data were stored on computer disk for subsequent analysis with custom-made computer analysis software. $V\dot{C}O_2$ and VT were expressed in mL body temperature and pressure, saturated (BTPS).

The study was performed in 21 normal subjects and 35 ambulatory COPD patients. Lung function data were obtained in the seated position with a flow-sensing spirometer (Fukuda; Spiroanalyzer ST300, Tokyo, Japan). Anthropometric and routine lung function data are given in table 1. Predicted values were those of MORRIS *et al.* [19]. The subjects were studied while seated, breathing room air through the mouthpiece apparatus with a noseclip on, at their own resting VT and respiratory frequency. Each subject had an initial 10–15 min trial run to become accustomed to the apparatus and procedure. After regular breathing had been achieved, a series of breaths over a period of 1 min were recorded. At the end of the recording time, while the subject was still connected to the mouthpiece, an arterial blood sample (>1 mL) was taken for gas analysis. An expert physician using a 21 G needle, performed a quick (5–10 s) and direct puncture of the brachial artery. It is highly unlikely that a change in blood gases took place in such a short time interval. If the procedure of gas sampling was not successful after one single effort, the experiment was cancelled. The cancelled experiments were <7.5%. The P_{a,CO_2} was measured with a blood gas analyser (CIBA-CORNING; 288 Blood gas system, MA, USA) in 12 normal subjects and in all COPD patients.

The method was experimentally verified in three normal subjects during tidal breathing through different tubes of a known capacity. The dead space of the added tube (V_{tube}) was calculated from the difference $V\text{D}$-$V\text{D(o)}$, where: $V\text{D}$ and $V\text{D(o)}$ are $V\text{D,Bohr}$ of the subject breathing through the mouthpiece apparatus with and without the added tube, respectively. Three tubes were used, the capacities (V_{cap}) of which were 180, 337 and 504 mL calculated from the equation $\pi\times r^2\times l$ (π=3.14, r=radius and l=length of the tube). The capacity of the tube deviated from the measured volume by <2.3% (table 2).

The study had the approval of the local ethics committee and all subjects gave informed consent.

Table 1. – Anthropometric and routine lung function data from 21 normal subjects and 35 chronic obstructive pulmonary disease (COPD) patients

	Normal subjects	COPD patients
Subjects n	21	35
Sex M/F	9/12	28/37
Age yrs	44±19	60±12
Weight kg	69±15	73±14
Height cm	168±10	167±9
FVC % pred	107±15	80±26
FEV1 % pred	106±13	57±28
FEV1/FVC %	82±6	55±14
FEF25–75 % pred	102±27	29±19

Values are presented as mean±SD or absolute number. M: male; F: female; FVC: forced vital capacity; FEV1: forced expiratory volume in one second; FEF25–75: forced mid-expiratory flow.

Table 2. – The capacity of the added tubes ($V_{cap}=\pi\times r^2\times l$), the mean of the measured volume (V_{tube}, measured) in three normal subjects, and the calculated volume (V_{tube}, calculated) obtained by the regression equation (footnote) are shown

Subjects	V_{cap} (n=3) mL	V_{tube}, measured mL	V_{tube}, calculated mL
1	180	176	178
2	337	341	339
3	504	509	510

V_{tube}, calculated$=-7.3751+1.0275\times V_{cap}$ (r=0.99).

Results

P_{A,CO_2} and $V_{D,Bohr}/V_T$ were measured by analysis of the V_{CO_2} *versus* V_T curve obtained from 21 normal subjects and 35 COPD patients during tidal breathing. It is noted that cardiogenic oscillations had no effect on the V_{CO_2} *versus* V_T curve, as this was consistently smooth in all subjects (Appendix 1). $V_{D,Bohr}/V_T$, V_T, P_{ET,CO_2} and P_{A,CO_2}, were obtained for each subject by averaging all breaths during a 1-min data recording period.

The mean within-study, within-day and day-to-day coefficient of variation for $V_{D,Bohr}/V_T$ was 6.5, 6.85 and 7.25% and for P_{A,CO_2} 1.57, 3.06, and 3.05%, respectively. These were determined in three normal subjects in whom measurements were repeated three times per day for 3 consecutive days.

$V_{D,Bohr}/V_T$ and $V_{D,phys}/V_T$ were not significantly different in the 12 normal subjects. In contrast, this difference was statistically significant in the COPD patients ($p<0.001$). The $V_{D,Bohr}/V_T$ ratio in COPD patients was significantly higher than in normal subjects ($p<0.001$), (table 3; fig. 1). $V_{D,Bohr}/V_T$ was higher than the dead space ratio measured from the F_{CO_2} *versus* V_T curve by Fowler's geometrical method of orthogonal projection ($V_{D(F)}/V_T$). In normal subjects, mean $\pm$ SD $V_{D(F)}/V_T$ was $28\pm8\%$ and in COPD patients, $37\pm8\%$. The mean difference between $V_{D,Bohr}/V_T$ and $V_{D(F)}/V_T$ is $5\pm1\%$ in normal subjects ($p<0.001$) and $7\pm2\%$ in COPD patients ($p<0.001$).

P_{A,CO_2} and P_{a,CO_2} were compared in 12 normal subjects and in all patients. In the COPD patients, P_{a,CO_2} was significantly higher than P_{A,CO_2} ($p<0.001$). In the 12 normal subjects, the difference between P_{a,CO_2} and P_{A,CO_2} was not statistically significant (table 4; fig. 2). In all normal subjects and patients, P_{A,CO_2} was significantly higher than P_{ET,CO_2} (table 4, fig. 3). The relationship between P_{ET,CO_2} and P_{A,CO_2} is shown in figure 3.

The alveolar-end-tidal P_{CO_2} ((A-ET) CO_2) and the arterial-alveolar P_{CO_2} ((a-A) CO_2) differences were also related to the $V_{D,Bohr}/V_T$ ratio. In all subjects, no statistical relationship was found between (a-A) CO_2

Table 3. – Comparison of dead space ratios, in 21 normal subjects and 35 chronic obstructive pulmonary disease (COPD) patients

Subject type	$V_{D,Bohr}/V_T$	$V_{D,phys}/V_T$	p-value
Normal subjects	0.333 ± 0.090	0.378 ± 0.088	p=0.135
COPD patients	0.436 ± 0.097	0.498 ± 0.123	$p<0.001$
p-value	$p<0.001$	p=0.003	

Mean values $\pm$ SD. $V_{D,Bohr}/V_T$: Bohr's dead space ratio; $V_{D,phys}/V_T$: physiological dead space ratio; p-value: indicate comparisons of respective rows/columns.

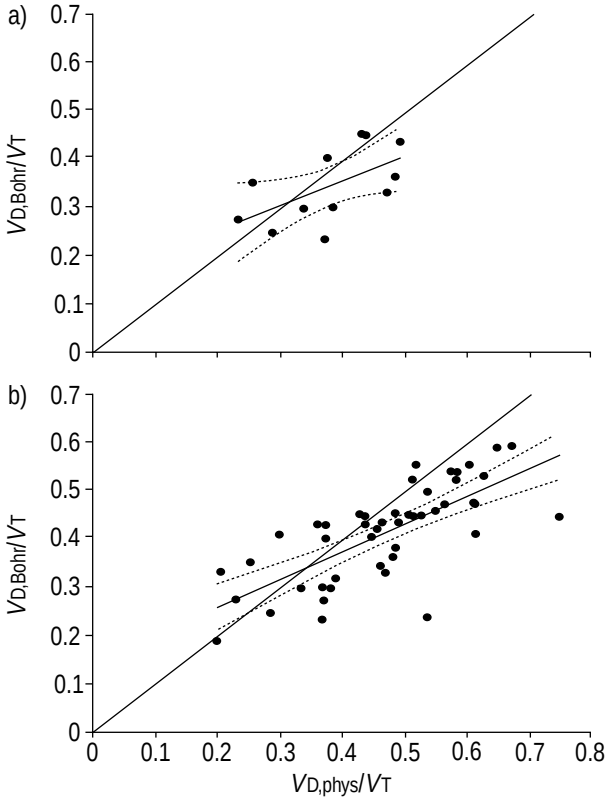

Fig. 1. – Scatter diagrams illustrating the relationship between Bohr's dead space ratio (Bohr's dead space/tidal volume ($V_{D,Bohr}/V_T$)) and physiological dead space ratio (physiological dead space/tidal volume ($V_{D,phys}/V_T$)) in a) normal subjects and b) chronic obstructive pulmonary disease patients. Regression lines are shown: a) $V_{D,Bohr}/V_T=0.151+0.508$ ($V_{D,phys}/V_T$), r=0.584, n=12, p=0.046; b) $V_{D,Bohr}/V_T=0.17+0.54$ ($V_{D,phys}/V_T$), r=0.691, n=35, $p<0.001$. Dotted lines represent 95% confidence intervals of regression.

Table 4. – Alveolar (P_{A,CO_2}) arterial (P_{a,CO_2}), and end-tidal (P_{ET,CO_2}) carbon oxide tension (kPa), in normal subjects and chronic obstructive pulmonary disease (COPD) patients

CO_2 tension variable	Normal subjects		COPD patients
Subjects n	21	12	35
P_{A,CO_2}	4.88 ± 0.48	4.84 ± 0.59	4.93 ± 0.93
P_{ET,CO_2}	4.60 ± 0.45	-	4.38 ± 0.84
P_{a,CO_2}	-	5.01 ± 0.50	5.54 ± 0.80
P_{A,CO_2}-P_{ET,CO_2}	0.28 ± 0.11	-	0.55 ± 0.22
P_{a,CO_2}-P_{A,CO_2}	-	0.17 ± 0.78	0.61 ± 0.83

Data are presented as mean $\pm$ SD.

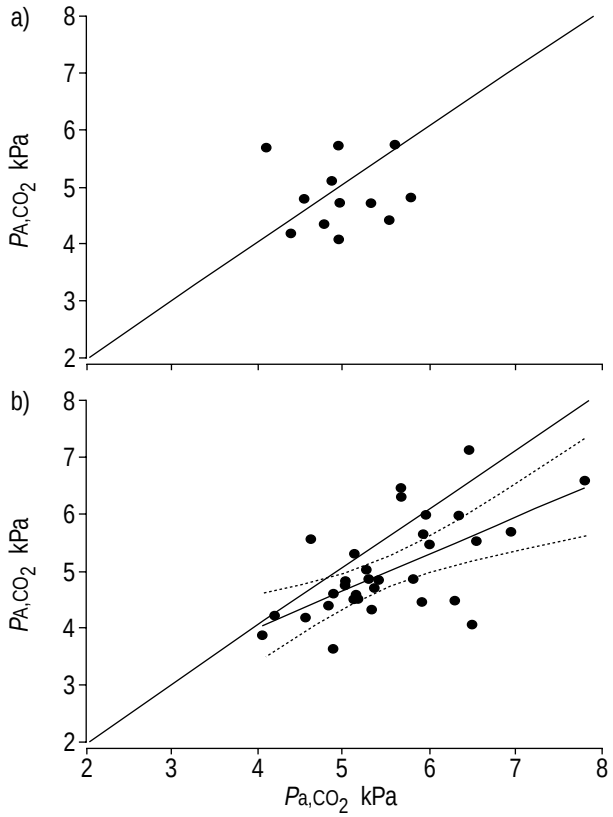

Fig. 2. – Scatter diagrams illustrating the relationship between alveolar (P_{A,CO_2}) and arterial carbon dioxide tensions (P_{a,CO_2}) in a) normal subjects and b) chronic obstructive pulmonary disease patients. A significant regression was found for COPD: P_{A,CO_2}=1.38+0.64 P_{a,CO_2}, r=0.551, n=35, $p<0.001$. Dotted lines represent 95% confidence intervals of regression.

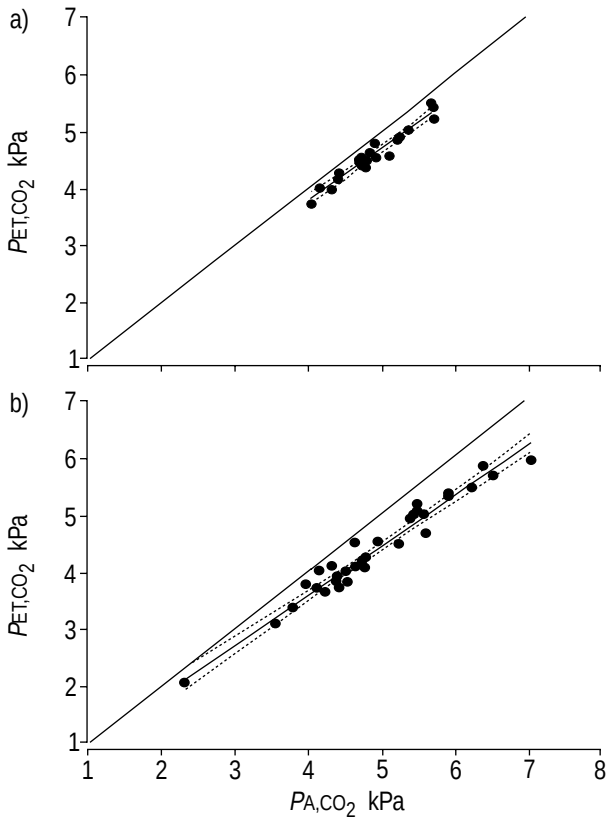

Fig. 3. – Scatter diagrams illustrating the relationship between end-tidal (P_{ET,CO_2}) and alveolar carbon dioxide (P_{A,CO_2}) tension in a) normal subjects and b) chronic obstructive pulmonary disease patients. Regression lines are shown: a) P_{ET,CO_2}=0.122+0.92 P_{A,CO_2}, r=0.972, n=21, $p<0.001$; b) P_{ET,CO_2}=0.065+0.88 P_{A,CO_2}, r=0.976, n=35, $p<0.001$. Dotted lines represent 95% confidence intervals of regression.

and $V_{D,Bohr}/V_T$. In contrast, the (A-ET) CO_2 was significantly related to the $V_{D,Bohr}/V_T$ ratio in both groups of subjects, *i.e.* (A-ET) CO_2=-0.050+($V_{D,Bohr}/V_T$) (kPa) (r=0.79, SEE=0.072, $p<0.001$) in normal subjects and (A-ET) CO_2=-0.261+1.852×($V_{D,Bohr}/V_T$) (kPa) (r=0.83, SEE=0.122, $p<0.001$) in COPD patients.

The validity of the analysis of the V_{CO_2} *versus* V_T curve was also examined by calculating the expired V_{CO_2} per breath from 1) the product F_{A,CO_2}×alveolar ventilation (V'_A) (=$V_{CO_2(A)}$), and 2) the equation $V_{CO_2(B)}=F_{sl}\times V_d+F_{ET,CO_2}\times$alveolar volume ($V_A$). The mean error between $V_{CO_2(A)}$ and $V_{CO_2(B)}$ was -0.02±1% in the normal subjects and 0.4±1% in the COPD patients (Appendix 3). The area $A_{(A)}$ differed from the area $A_{(B)}$ by 4±0.5% in normal subjects and 3±2% in COPD patients (Appendix 3).

Discussion

The present study used the expired V_{CO_2} *versus* the exhaled V_T curve for the noninvasive measurement of $V_{D,Bohr}/V_T$ and mean P_{A,CO_2} in normal subjects and COPD patients during tidal breathing. According to the results: 1) $V_{D,Bohr}/V_T$ is increased in COPD patients as compared to normal subjects; 2) $V_{D,Bohr}/V_T$ is lower than $V_{D,phys}/V_T$ in COPD patients; 3) P_{A,CO_2} is closely similar to P_{a,CO_2} in normal subjects, whilst it is significantly lower than P_{a,CO_2} in COPD patients; and 4) P_{A,CO_2} is significantly higher than P_{ET,CO_2} in all subjects, especially in COPD patients. This curve overcomes: 1) the assumption inherent in the analysis of the F_{CO_2} *versus* V curve, *i.e.* that F_{A,CO_2} is equal to F_{ET,CO_2}; and 2) the difficulty in drawing the extrapolated line of the sloping alveolar plateau in disease, especially during tidal breathing.

At a steady state, regardless of the actual value of the V'_A/perfusion (Q') ratio, the CO_2 molecules within the residual air define F_{A,CO_2}. This is dependent on the dynamic equilibrium within the alveolar space between the inflow and outflow of the CO_2 molecules, and the overall V'_A/Q' ratio of the lungs at the existing functional residual capacity. A portion of the CO_2 molecules is exhaled with the V_T constituting the expired V_{CO_2} per breath. During expiration, these molecules move out from the alveolar space mainly by bulk movement but also by diffusion, and at the same time they are replaced by CO_2 molecules originating from blood through the alveolar membrane. The concentrations of the CO_2 molecules within the airways, diluted by pre-inspired atmospheric air, are lower than the alveolar concentration. As a result of

the "dilution effect", the V_{CO_2} *versus* V_T curve gets the curvilinear shape recorded at the mouth (Appendix 1).

The analytical procedure of the V_{CO_2} *versus* V_T curve was verified, both theoretically and practically *i.e.* 1) The measurement of the volume of the added tubes with a deviation of $<2.3\%$ from the capacity of the tubes denotes the validity and the accuracy of the described method. The added tube affects the entire V_{CO_2} *versus* V_T curve and its volume was calculated from the change of $V_{D,Bohr}$. 2) The nonsignificant difference in normal subjects between P_{A,CO_2} and P_{a,CO_2} is strong evidence for the accuracy of the method. 3) The Equations 9 and 10 in Appendix 1, derived from the V_{CO_2} *versus* V_T curve, are identical to those widely accepted in the literature [1 – 18]. 4) The mean error between $V_{CO_2(A)}$ and $V_{CO_2(B)}$ is $<0.4\%$, *i.e.* $V_{CO_2(A)}=V_{CO_2(B)}$. This equality means that the points *b*, *d* and *a* are correctly positioned and not arbitrarily taken (Appendix 1, 3). Furthermore, the mean deviation of the area A(A) from the area A(B) is very small (Appendix 3).

The repeatability of the measurements for $V_{D,Bohr}/V_T$ was $\sim 7\%$ and for P_{A,CO_2} $\sim 3\%$. However, the increase of the coefficient of variation of the V_T *per se* beyond the value of 16% reduces the repeatability especially of $V_{D,Bohr}/V_T$.

$V_{D,Bohr}$(=segment *ia*; Appendix 1) is higher than $V_{D(F)}$, measured from the F_{CO_2} *versus* V curve (Fowler's method), by the amount of the volume segment V_{da} ($=V_{CO_2(d)}/F_{ET,CO_2}$), if the analysis of the F_{CO_2} *versus* V curve is performed according to the method of orthogonal projection of the curve (Appendix 2). So, the ratio $V_{D,Bohr}/V_T$ is higher than usually referred to in the literature [1 – 18]. If, however, the F_{CO_2} *versus* V curve is analysed by the method of the "sloping alveolar plateau", the difference between $V_{D,Bohr}$ and $V_{D(F)}$ is even higher (Appendix 2).

The alveolar CO_2 and the mixed expired CO_2 concentrations are the two ends of a spectrum of gas fractions influenced by several mechanisms affecting the homogeneity of ventilation. According to the law of conservation of mass, the product $F_{E,CO_2}\times V_T$ is equal to $F_{A,CO_2}\times V_A$ or to the intermediate products $F_{sl}\times V_{be}$ or $F_{ET,CO_2}\times V_{de}$ (Appendix 1). That is, V_{CO_2} per breath is exhaled with the V_T at the mixed expired gas concentration or with smaller volumes at increased gas concentrations until the minimal volume (alveolar, V_A) at the highest gas concentration (F_{A,CO_2}). Mean F_{A,CO_2} cannot be greater than a maximal value determined by the overall V'_A/Q' ratios of the lungs.

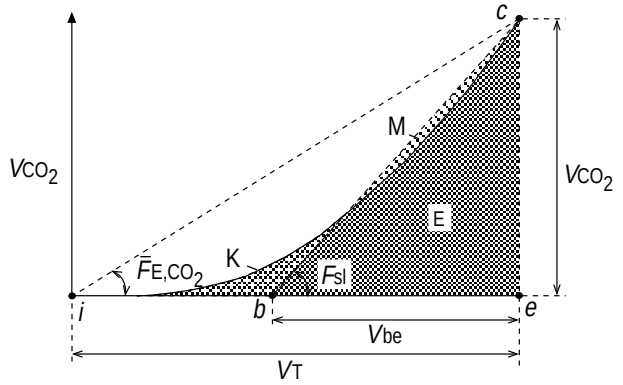

Fig. 4. – The expired carbon dioxide (CO_2) volume *versus* the exhaled volume curve (V_{CO_2} *versus* V_T) obtained from a chronic obstructive pulmonary disease patient. The volume segment *ie* is the tidal volume (V_T). The point *I* is the beginning of expiration and the point *e* the end of it. Angle *cie* is the mixed expired CO_2 concentration (F_{E,CO_2}). Angle *cbe* (F_{sl}) is the average slope of the curve. The area under the whole curve (area E) is equal to the area of the triangle *cbe*. The areas K and M are equal to each other. V_{be}: volume segment *be*.

The real V_{CO_2} *versus* V_T curve functionally can be represented by the line *iac* (Appendix 1). The segment *ia* is $V_{D,Bohr}$, which if considered without CO_2 gas, then the segment *ae* (=projection of the line *ac* on the horizontal axis with the angle *cae* ($=F_{A,CO_2}$)) is the mean V_A transferring out all the V_{CO_2} per breath with the maximal concentration (F_{A,CO_2}).

$V_{D,Bohr}/V_T$ is considered as an index of maldistribution of the expired air within the lungs, *i.e.* within the space between the inner surface of the alveolar membrane and the mouth. The $V_{D,phys}/V_T$ is influenced not only by the mechanisms of uneven ventilation, but also by the mechanisms of inhomogeneous distribution of Q'. In normal subjects, in whom P_{a,CO_2} is approximately equal to P_{A,CO_2}, the difference between $V_{D,phys}/V_T$ and $V_{D,Bohr}/V_T$ was not statistically significant. This may be a true result or is more likely due to the small number of observations (power of paired t-test=0.201). In the COPD patients, in whom P_{a,CO_2} was higher than P_{A,CO_2}, the difference between the two dead space ratios was considerable (table 3).

P_{a,CO_2} in normal subjects was not significantly different from P_{A,CO_2}. However, in COPD patients (a-A) CO_2 was significantly higher than in normal subjects (table 4). This may be explained as follows. An increased P_{A,CO_2} in regions with low V'_A/Q' ratio is followed by an increase of the end-capillary P_{CO_2} (P_{c,CO_2}) locally, while in regions with a high V'_A/Q' ratio, the decrease of P_{A,CO_2} is accompanied by a local decrease of P_{c,CO_2}. If the arterial blood is composed mainly from blood perfusing regions with a low V'_A/Q' ratio, P_{a,CO_2} will be increased. At the same time, when the exhaled V_T contains air coming mostly from regions with high V'_A/Q' ratio, P_{A,CO_2} will be decreased. The combination of these two conditions probably results in the increased (a-A) CO_2 in patients with COPD. This is compatible with the results obtained, *i.e.* that the (a-A) CO_2 is not statistically related to $V_{D,Bohr}/V_T$ in the subjects studied. In contrast, (A-ET) CO_2 is significantly related to $V_{D,Bohr}/V_T$ in all subjects, due to the existing inhomogeneity of ventilation, especially in the COPD patients. The (A-ET) CO_2 was higher in COPD patients than in normal subjects (table 4). In addition, P_{A,CO_2} was linearly related to P_{ET,CO_2}, and P_{A,CO_2} was higher than P_{ET,CO_2} in all subjects (fig. 3). The (A-ET) CO_2 difference was strongly related to $V_{D,Bohr}/V_T$ in normal subjects and COPD patients, as is described in Equation 11 (Appendix 1).

P_{A,CO_2} is V_{CO_2}/V_A times the factor (barometric

pressure-47), as conventionally referred to in the literature. It is mentioned that the measured value of P_{A,CO_2} per breath is a mean value from all the regions of the lungs with different $V'A/Q'$ ratios. Furthermore, the values of P_{A,CO_2} shown in the Results section are mean values from all breaths during the 1-min sampling period.

It is concluded that the carbon dioxide output *versus* tidal volume curve obtained during tidal breathing with minimal cooperation on the patient's part, is useful in clinical practice and research work. It allows, with accuracy and precision, the noninvasive measurement and monitoring of the mean alveolar carbon dioxide tension and Bohr's dead space volume. The alveolar carbon dioxide tension can be safely used instead of the arterial one in normal subjects, but not in chronic obstructive pulmonary disease patients. In all subjects, end-tidal carbon dioxide tension cannot be used instead of alveolar carbon dioxide tension.

Appendix

1. The expired carbon dioxide volume versus *tidal volume curve*

The simplified analysis of the $V\mathrm{CO_2}$ *versus* $V\mathrm{T}$ curve, presented in geometrical terms, is as follows. The total area under the $V\mathrm{CO_2}$ *versus* $V\mathrm{T}$ curve (E) is equal to the area of the triangle *bce*. In either side of the line *bc* (hypotenuse) the areas K and M are equal to each other (fig. 4). Accordingly, the volume segment *be* ($V\mathrm{be}$) on the $V\mathrm{T}$ axis is equal to (fig. 5):

$$V_{be} = 2E / V_{CO_2} \quad (1)$$

The angle *cbe* represents the average slope ($F\mathrm{sl}=V\mathrm{CO_2}/V\mathrm{be}$) of the $V\mathrm{CO_2}$ *versus* $V\mathrm{T}$ curve (figs. 4 and 5). F_{ET,CO_2} is measured directly at the end of the $F\mathrm{CO_2}$ *versus* time curve. The ratio $V\mathrm{CO_2}/F_{ET,CO_2}$ determines the volume segment *de* ($V\mathrm{de}$) on the horizontal axis (fig. 5), *i.e.*

$$V_{de} = V_{CO_2} / F_{ET,CO_2} \quad (2)$$

The line *cd*, the volume segment *id* and the curve itself confine the one-sided area D, which is equal to the area of the triangle *bcd* (fig. 5), *i.e.*

$$D = \frac{1}{2} V_{CO_2} \times (V_{be} - V_{de}) \quad (3)$$

where: (Vbe-Vde) is the base (volume segment *bd*=Vd) of the triangle *bcd*. The area D denotes that a part of $V\mathrm{CO_2}$ ($V\mathrm{CO_2(d)}$) is exhaled at smaller concentrations than F_{ET,CO_2}. The gas volume $V\mathrm{CO_2(d)}$ (segment *xd*) is calculated from the average slope of the curve (Fsl) and the volume segment Vd (fig. 5), *i.e.*

$$V_{CO_2(d)} = F_{sl} \times V_d \quad (4)$$

The gas volume $V\mathrm{CO_2}$, as already described, is expired in two parts, the initial one ($V\mathrm{CO_2(d)}$) with a mean concentration Fd and the rest ($V\mathrm{CO_2}$-$V\mathrm{CO_2(d)}$) with concentration equal to F_{ET,CO_2} (fig. 6). The meeting point (y) of these two slopes (Fd and F_{ET,CO_2})

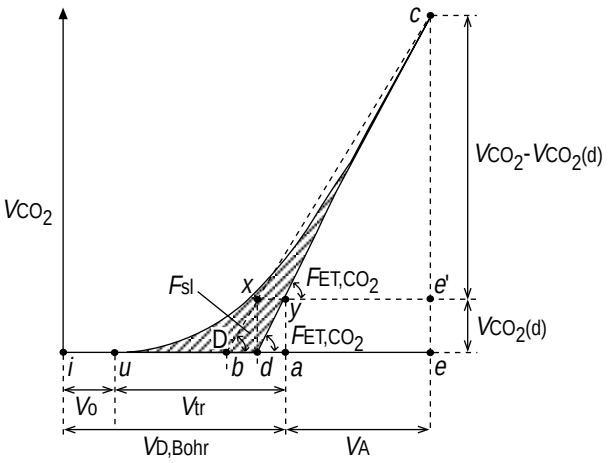

Fig. 5. – The same curve as in figure 4. The slope of the line *cd* represents the end-tidal concentration (F_{ET,CO_2}), measured directly from the carbon dioxide fraction ($F\mathrm{CO_2}$) *versus* time curve. Area D is equal to the area of the triangle *bcd* ($=\frac{1}{2}V\mathrm{CO_2}\times V$d), where $V\mathrm{CO_2}$ is expired CO_2 and Vd is the volume segment *bd* ($=V$be-Vde). The gas volume $V\mathrm{CO_2(d)}$ (=gas volume segment *xd*=*ya*=*ee'*) is calculated from Equation 4. The segment *iu* contains no CO_2 gas ($=V$o) and it represents the upper airways dead space volume. The volume segment *ua* represents the transitional volume (Vtr). VD,Bohr: Bohr's dead space; VA: alveolar ventilation.

lies on the line *cd* and the gas volume segments *xd*, *ya* and *ee'* are equal to each other ($=V\mathrm{CO_2(d)}$) (figs. 5 and 6). The volume segment *ye' is* equal to the segment *ae*, and represents the alveolar part of the $V\mathrm{T}$ with which the gas volume ($V\mathrm{CO_2}$-$V\mathrm{CO_2(d)}$) is expired at the end-tidal concentration (F_{ET,CO_2}), *i.e.*

$$V_A = (V_{CO_2} - V_{CO_2(d)}) / F_{ET,CO_2} \quad (5)$$

VD,Bohr is equal to:

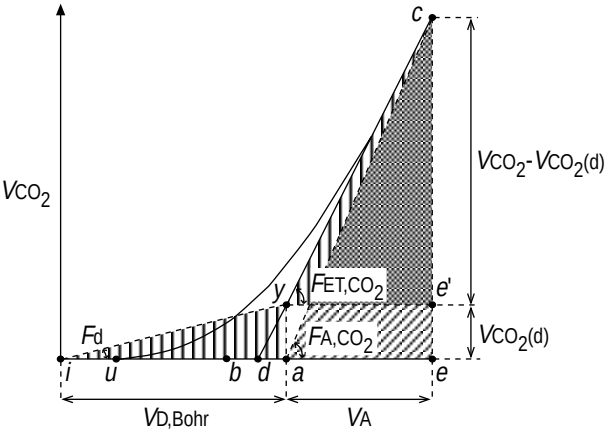

Fig. 6. – The same curve as in figure 4. The point *y* on the line *cd* is the limit, below which the gas volume is expired at the mean concentration Fd ($=V\mathrm{CO_2(d)}/(V$D,Bohr)) (smaller than end-tidal carbon dioxide fraction (F_{ET,CO_2})) and above which at a constant concentration equal to F_{ET,CO_2}. The segment *yc* projected horizontally with the slope F_{ET,CO_2} gives the volume segment *ye'*, which is equal to the volume segment *ae* representing the alveolar volume (VA). The triangular area *cae* is equal to the sum of the areas *iya* and *cye'*. $V\mathrm{CO_2}$ per breath forms with the VA the angle *cae*, which represents the mean alveolar CO_2 concentration (F_{A,CO_2}). The volume segment *ia* represents Bohr's dead space volume (VD,Bohr).

$$V_{D,Bohr} = V_T - V_A \quad (6)$$

This is divided into two portions, the initial volume V_o (=volume segment *iu*) and the transitional volume V_{tr} (=volume segment *ua*) (figs. 5 and 6). The volume V_o is the initial part of the V_T with no CO_2 gas in it. The transitional volume contains the gas volume $V_{CO_2(d)}$ and is equal to (figs. 5 and 6):

$$V_{tr} = V_T - V_o - V_A \quad (7)$$

and

$$V_{tr}/V_T = 1 - (V_o/V_T) - (V_A/V_T) \quad (8)$$

The volume V_o is directly measured by the computer as the volume segment from the beginning of expiration (point *i*) to point *u*, at which CO_2 gas starts appearing in the expired air.

V_A is calculated from Equation 5. If F_{CO_2} is considered as zero in $V_{D,Bohr}$ (V_o+V_{tr}), then all the V_{CO_2} per breath should be expired with the V_A (fig. 6). So, the mean alveolar F_{CO_2} is calculated from the equation:

$$F_{A,CO_2} = V_{CO_2}/V_A \quad (9)$$

By substituting in Equation 9 the term V_{CO_2} by its equal $F_{E,CO_2} \times V_T$, the equation for the V_A/V_T ratio is the following:

$$V_A/V_T = F_{E,CO_2}/F_{A,CO_2} \quad (10)$$

where F_{E,CO_2} is the mixed expired CO_2 fraction (=($\Sigma o^n(dV_{CO_2}/dV)$]/n=angle *cie*) (fig. 4). Since the V_A is smaller than the volume segment V_{de} by the volume segment *da* ($V_{da}=V_{CO_2(d)}/F_{ET,CO_2}$), F_{A,CO_2} is greater than F_{ET,CO_2} (fig. 6), *i.e.*

$$F_{A,CO_2} - F_{ET,CO_2} = V_{CO_2}(d)/V_A \quad (11)$$

Equation 11 is derived from Equations 5 and 9.

2. *Relationship between the expired carbon dioxide* versus *tidal volume and carbon dioxide fraction* versus *tidal volume*

The gas volume *versus* V_T curve (lower curve) and the corresponding gas concentration *versus* V_T curve (upper curve) are obtained from a single breath of a COPD patient (fig. 7). In the upper curve (F_{CO_2} *versus* V_T curve), the vertical line *dd'* corresponds to the point *d* of the lower curve. The line *dd'* separates the F_{CO_2} *versus* V_T curve to the areas A and B, which are equal to each other. It is evident that $V_{D(F)}$, measured by Fowler's technique of orthogonal projection, is smaller than $V_{D,Bohr}$ by the volume segment V_{da}. It is mentioned that if $V_{CO_2(d)}$ is zero, $V_{D(F)}$ is equal to $V_{D,Bohr}$. In the upper curve (F_{CO_2} *versus* V_T), the drawing of the line of the "sloping alveolar plateau" is very difficult. However, if the last part of the F_{CO_2} *versus* V_T, which by no means is a straight line, is extrapolated, $V_{D(F)}$ becomes even smaller as compared to $V_{D,Bohr}$ by the volume segment V_{da} (fig. 7).

3. *Verification of the method*

The analysis of the V_{CO_2} *versus* V_T curve was verified as follows: 1) In three normal subjects breathing tidally through tubes of known capacity (V_{cap}) interposed between the mouthpiece and the monitoring ring, the dead space volume was measured without ($V_{D(o)}$) and with the added tube (V_D). The difference V_D-$V_{D(o)}$ was compared with the capacity of the added tube (Results). 2) The gas volume $V_{CO_2(A)}$ (=$F_{A,CO_2} \times V_A$) was compared to the volume $V_{CO_2(B)}$ (=$F_{sl} \times V_d + F_{ET,CO_2} \times V_A$) (fig. 6). The error between $V_{CO_2(A)}$ and $V_{CO_2(B)}$ was calculated from (l-($V_{CO_2(B)}/V_{CO_2(A)}$))×100 (Results). 3) The area A(A) (=$^1/_2 V_A \times V_{CO_2}$) was compared to the area A(B) (=$^1/_2 V_{D,Bohr} \times V_{CO_2(d)} + ^1/_2 V_A \times (V_{CO_2} - V_{CO_2(d)})$) with an

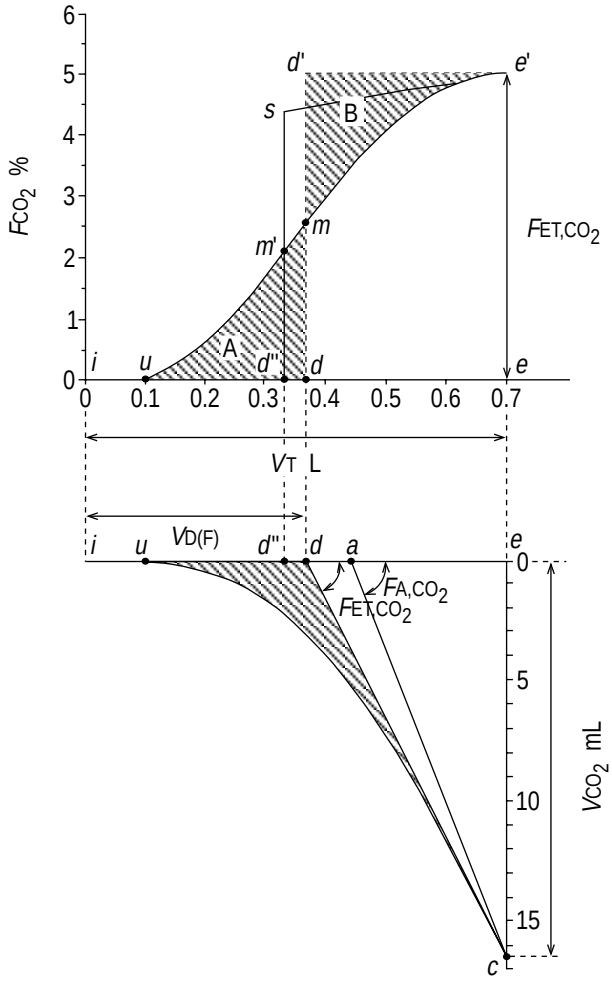

Fig. 7. – The carbon dioxide concentration *versus* the exhaled volume curve (F_{CO_2} *versus* V_T) (upper curve) obtained from a chronic obstructive pulmonary disease patient and the expired CO_2 *versus* exhaled volume (V_{CO_2} *versus* V_T) curve (lower curve), which is derived from the upper curve. F_{CO_2} is expressed in %, V_T in litres, and V_{CO_2} in mL. In this patient, Bohr's dead space ratio (Bohr's dead space/tidal volume ($V_{D,Bohr}/V_T$)) is 0.60. According to the geometrical method of orthogonal projection, anatomical dead space measured by Fowler's technique/tidal volume ratio ($V_{D(F)}/V_T$) is equal to 0.53. If the extrapolation of the "sloping alveolar plateau" is drawn, the ratio $V_{D(F)}/V_T$ becomes even smaller than when measured by the technique of orthogonal projection and is equal to 0.48.

error calculated from $[1-(A_{(B)}/A_{(A)})]\times 100$ (Results) (fig. 6). 4) In normal subjects, P_{A,CO_2} did not differ significantly from P_{a,CO_2} (Results).

Acknowledgements. The authors are grateful to N.B. Pride, M. Hughes, and P.T. Macklem for their most constructive criticism.

References

1. Bohr C. Ueber die lungeatmung. *Skand Arch Physiol* 1891; 2: 236–238.
2. Enghoff H. Volumen inefficax, Bemerkungen zur Frage des schadlichen. *Raumes Ups Lakaref* 1938; 44: 191–218.
3. Riley RL, Lilienthal JL, Proemmel DD, Franke RE. On the determination of the physiologically effective pressures of oxygen and carbon dioxide in alveolar air. *Am J Physiol* 1946; 147: 191–198.
4. Fowler WS. Lung function studies II. The respiratory dead space. *Am J Physiol* 1948; 154: 405–416.
5. Fowler WS. Lung function studies III. Uneven pulmonary ventilation in normal subjects and in patients with pulmonary disease. *Am J Physiol* 1949; 2: 283–299.
6. Asmussen E, Nielsen M. Physiological dead space and alveolar gas pressures at rest and during muscular exercise. *Acta Physiol Scand* 1956; 38: 1–21.
7. Bouhuys A. Respiratory dead space. *In*: Fenn WO, Rahn H, eds. Respiration. American Physiological Society, 1964; pp. 699–714.
8. Otis AB. Quantitative relationships in steady-state gas exchange. *In*: Fenn WO, Rahn H, eds. Respiration. American Physiological Society, 1964; pp. 681–698.
9. Sykes MK, McNicol MW, Campbell EJM. Respiratory failure. Blackwell Science Publication, Oxford, 1969; pp. 51–314.
10. Hugh-Jones P, Barter CE, Hime JM, Rusbridge MM. Dead space and tidal volume of the giraffe compared with some other mammals. *Respir Physiol* 1978; 35: 53–58.
11. Luft UC, Loeppky JA, Mostyn EM. Mean alveolar gases and alveolar-arterial gradients in pulmonary patients. *J Appl Physiol* 1979; 46: 534–540.
12. Engel LA. Intraregional gas mixing and distribution. *In*: Engel LA, Paiva M, eds. Gas mixing and distribution in the lung. Marcel Dekker, New York, 1985; pp. 326–327.
13. Anthonisen NR, Fleetman JA. Ventilation: total, alveolar, and dead space. *In*: Fishman AP, Fahri LE, Tenney RM, Geigen SR, eds. Handbook of Physiology, The respiratory system. American Physiological Society, 1987; pp. 113–129.
14. Hlastala MP. Ventilation. *In*: Crystal RG, West JB, Barnes PJ, eds. Raven Press, New York, 1991; pp. 1211–1213.
15. Cerretelli P, di Prampero PE. Pulmonary gas exchange. *In*: Crystal RG, West JB, Barnes PJ, Cherniack NS, Weibel ER, eds. The lung. 1st Edn. Raven Press, New York, 1991; pp. 1565–1572.
16. Tenney SM, Miller RM. Dead space ventilation in old age. *J Appl Physiol* 1956; 9: 321–327.
17. Jordanoglou J, Koulouris N, Kyroussis D, Rapakoulias P, Vassalos P, Madianos J. Measurement of effective alveolar carbon dioxide tension during spontaneous breathing in normal subjects and patients with chronic airways obstruction. *Thorax* 1995; 50: 240–244.
18. Jordanoglou J, Tatsis G, Danos J, Gougoulakis S, Orfanidou D, Gaga M. Alveolar partial pressures of carbon dioxide and oxygen measured by a helium washout technique. *Thorax* 1990; 45: 520–524.
19. Morris MJ, Koski A, Johnson LC. Spirometric standards for healthy non-smoking adults. *Am Rev Respir Dis* 1971; 103: 57–67.